Discovery of an integrative network of microRNAs and transcriptomics changes for acute kidney injury

Chan Gyu Lee[1], Jin Geol Kim[1], Hyun Joo Kim[1], Hyuk-Kwon Kwon[2], Il Je Cho[3], Dal Woong Choi[4], Woo Hyung Lee[1], Won Dong Kim[1], Se Jin Hwang[5], Sangdun Choi[2] and Sang Geon Kim[1]

[1]Research Institute of Pharmaceutical Sciences, College of Pharmacy, Seoul National University, Seoul, Korea; [2]Department of Molecular Science and Technology, Ajou University, Suwon, Korea; [3]College of Oriental Medicine, Daegu Haany University, Daegu, Korea; [4]Department of Public Health Science, Graduate School, College of Health Sciences, Korea University, Seoul, Korea and [5]College of Medicine, Hanyang University, Seoul, Korea

The contribution of miRNA to the pathogenesis of acute kidney injury (AKI) is not well understood. Here we evaluated an integrative network of miRNAs and mRNA data to discover a possible master regulator of AKI. Microarray analyses of the kidneys of mice treated with cisplatin were used to extract putative miRNAs that cause renal injury. Of them, miR-122 was mostly downregulated by cisplatin, whereas miR-34a was upregulated. A network integrating dysregulated miRNAs and altered mRNA expression along with target prediction enabled us to identify Foxo3 as a core protein to activate p53. The miR-122 inhibited Foxo3 translation as assessed using an miR mimic, an inhibitor, and a Foxo3 3′-UTR reporter. In a mouse model, Foxo3 levels paralleled the degree of tubular injury. The role of decreased miR-122 in inducing Foxo3 during AKI was strengthened by the ability of the miR-122 mimic or inhibitor to replicate results. Increase in miR-34a also promoted the acetylation of Foxo3 by repressing Sirt1. Consistently, cisplatin facilitated the binding of Foxo3 and p53 for activation, which depended not only on decreased miR-122 but also on increased miR-34a. Other nephrotoxicants had similar effects. Among targets of p53, Phlda3 was robustly induced by cisplatin, causing tubular injury. Consistently, treatment with miR mimics and/or inhibitors, or with Foxo3 and Phlda3 siRNAs, modulated apoptosis. Thus, our results uncovered an miR integrative network regulating toxicant-induced AKI and identified Foxo3 as a bridge molecule to the p53 pathway.

Kidney International (2014) **86,** 943–953; doi:10.1038/ki.2014.117; published online 23 April 2014

KEYWORDS: acute kidney injury; cell death; microarray analysis; miRNA expression; pathophysiology of renal disease; progression

Correspondence: *Sang Geon Kim, Research Institute of Pharmaceutical Sciences, College of Pharmacy, Seoul National University, Gwanakno 599, Seoul 151-742, Korea. E-mail: sgk@snu.ac.kr*

Received 13 August 2013; revised 9 February 2014; accepted 6 March 2014; published online 23 April 2014

Acute kidney injury (AKI), which is most commonly caused by nephrotoxicants, markedly increases morbidity and mortality in hospitalized patients.[1,2] A variety of chemicals such as drugs and environmental materials can induce AKI.[3] Drugs have an ongoing etiological role in the occurrence of nephropathy for their direct damaging action on tubular cells. It is recognized as the most common cause of kidney-related problems because nontoxic concentration of the drug during treatment could reach toxic levels in the kidney. In particular, renal tubular cells are vulnerable to the toxic effects of drugs because of their role in concentrating and reabsorbing the glomerular filtrate. Despite the ongoing studies, prevalence of drug-induced AKI remains significantly high. As chemical-induced nephropathy accompanies the disruption of certain signal transduction pathways, understanding of the signaling and working molecules would be of value in finding a way to prevent toxicity and/or treat kidney injury.

The microRNA (miRNA) negatively regulates gene expression by base-pairing with the 3′-untranslated region (UTR) of target messenger RNA.[4] Abnormal levels of miRNA could be one of the mechanisms explaining dysregulated protein expression during kidney disease progression.[5] Although profiles of miRNA expression have been examined in renal diseases, such as polycystic disease, diabetic nephropathy, renal cancer, and fibrosis,[6–9] few studies have specifically described the identification of miRNAs and their roles in AKI. Moreover, little information was available on the network integrating miRNA dysregulation and altered mRNA expression that occur in nephropathy. Considering the fact that the correlation between transcriptome and proteome expression is not always linear because of posttranscriptional regulation of mRNA translation and protein modifications,[10] an integrative network of both miRNA and mRNA databases may provide key information in identifying the factors involved in drug-induced toxicity, shedding light on new strategies for the management of AKI.

Drugs such as cisplatin, aminoglycosides, and amphotericin B induce tubular injury. In particular, cisplatin is a widely prescribed agent; its main dose-limiting side effect is

AKI itself, and it is a direct inducer of proximal and distal tubular epithelial cell damage. Nephrotoxicity of cisplatin is a composite result of many presentations implicated in drug-induced nephrotoxicity, such as drug transport, activation of multiple pathways, and initiation of inflammatory response,[11] which makes cisplatin a suitable model for AKI.

This study investigated an integrative regulatory network of altered miRNA and transcript levels governing AKI induced by cisplatin treatment. In particular, we were interested in identifying the specific miRNAs that directly control a bridge molecule leading to cell death during AKI. Of the miRNAs differentially expressed in the miRNA microarrays, we found the most significant reciprocal changes in the levels of miR-122 and -34a during renal injury. Moreover, we identified their coordinated translational and posttranslational roles in activating Foxo3 as a molecule bridging to p53-dependent apoptosis. To assess the degree of nephropathy, a cascade of cell death pathway, and the underlying basis, both animal and cell models were utilized along with a bioinformatic approach using the outcomes of miRNA and mRNA microarrays. In addition, our findings uncovered the functional role of Phlda3, an effector molecule substantially induced downstream of p53, in tubular cell death.

RESULTS

miRNAs dysregulated in AKI caused by cisplatin

To identify the miRNAs dysregulated in AKI induced by cisplatin, renal miRNA microarray analyses were carried out in mice at day 3 after a single intraperitoneal (i.p.) injection of cisplatin (15 mg/kg). Seven miRNAs showed significant changes in expression on cisplatin treatment when a cutoff of $P<0.05$ was used; the expression of five was decreased, whereas that of two was increased (Figure 1a). Of them, miR-122 levels showed the greatest downregulation compared with vehicle-treated control, whereas expression of miR-34a was distinctly increased. Quantitative reverse transcription-PCR assays confirmed the changes (Figure 1b). In the time-course study, miR-122 levels decreased on day 1 after cisplatin treatment and remained low until day 3. At day 5, they were slightly increased from the trough (Figure 1c, left). However, miR-34a levels increased significantly at day 3 and were further increased at day 5 after treatment (Figure 1c, right). In a subsequent study, we narrowed our focus on dysregulation of miR-122 and -34a because the changes were the greatest.

a

Log2 (Cisplatin/vehicle) ratio of differentially expressed miRNAs that reached statistical significance by T-test ($P < 0.05$)

Downregulated miRNAs			Upregulated miRNAs		
miRNA	Log2 ratio	*P*-value	miRNA	Log2 ratio	*P*-value
miR-122	–3.39	0.0326	miR-34a	1.11	0.0213
miR-10b*	–1.16	0.0428	let-7g	0.27	0.0420
miR-30e	–0.44	0.0363			
miR-193	–0.26	0.0363			
miR-26a	–0.31	0.0293			

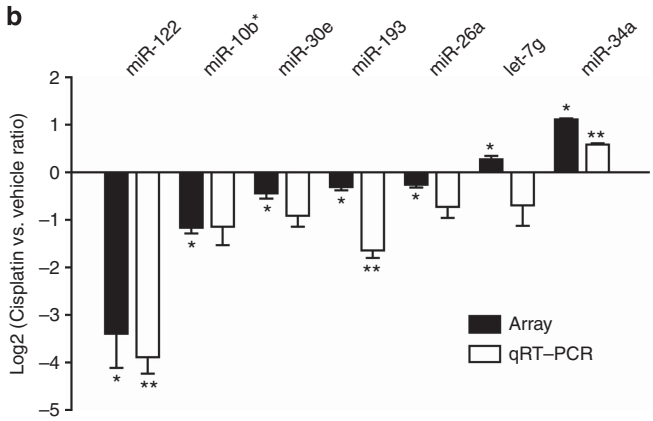

Figure 1 | The expression profiles of microRNAs (miRNAs) in the kidney after cisplatin treatment. (**a**) A list of differentially expressed miRNAs in the microarray analysis, including log2 ratio and *P* values. Microarrays were performed with miRNA samples extracted from the kidney at day 3 after a single administration of vehicle or cisplatin (15 mg/kg) to C57BL/6 mice. (**b**) Quantitative reverse transcription PCR (qRT-PCR) validation of differentially expressed miRNAs. Results are shown as mean of log2(cisplatin/vehicle) and are presented side-by-side with the respective array results. (**c**) The effects of cisplatin treatment on the levels of miR-122 and -34a. For **b** and **c**, values represent the mean ± s.e.m. (significantly different as compared with vehicle treatment according to array or qRT-PCR analysis, respectively, $*P<0.05$, $**P<0.01$; $N=3$ per group in miRNA array and $N=4$ per group in qRT-PCR).

An integrated regulatory network of dysregulated miRNAs and mRNAs

To facilitate the prediction of targets possibly interacting with miR-122 and -34a, we performed cDNA microarray analyses using the kidneys of mice treated with a single dose of cisplatin (15 mg/kg, at day 3), and the microarray profiles were compared (Figure 2a). Among those represented on the microarray, 36 genes were differentially expressed by cisplatin treatment when $P<0.01$ and a twofold change cutoff were used. Bioinformatic analyses using TargetScan algorithms allowed us to select the targets putatively regulated by miR-122 and -34a. In this approach, we focused on five candidate genes that have potential to be regulated by decreased miR-122 in association with cell death (Supplementary Table S1 online). Twelve genes were chosen as possible targets affected by increased miR-34a (Supplementary Table S2 online). Integrated analyses of miRNA and mRNA expression data

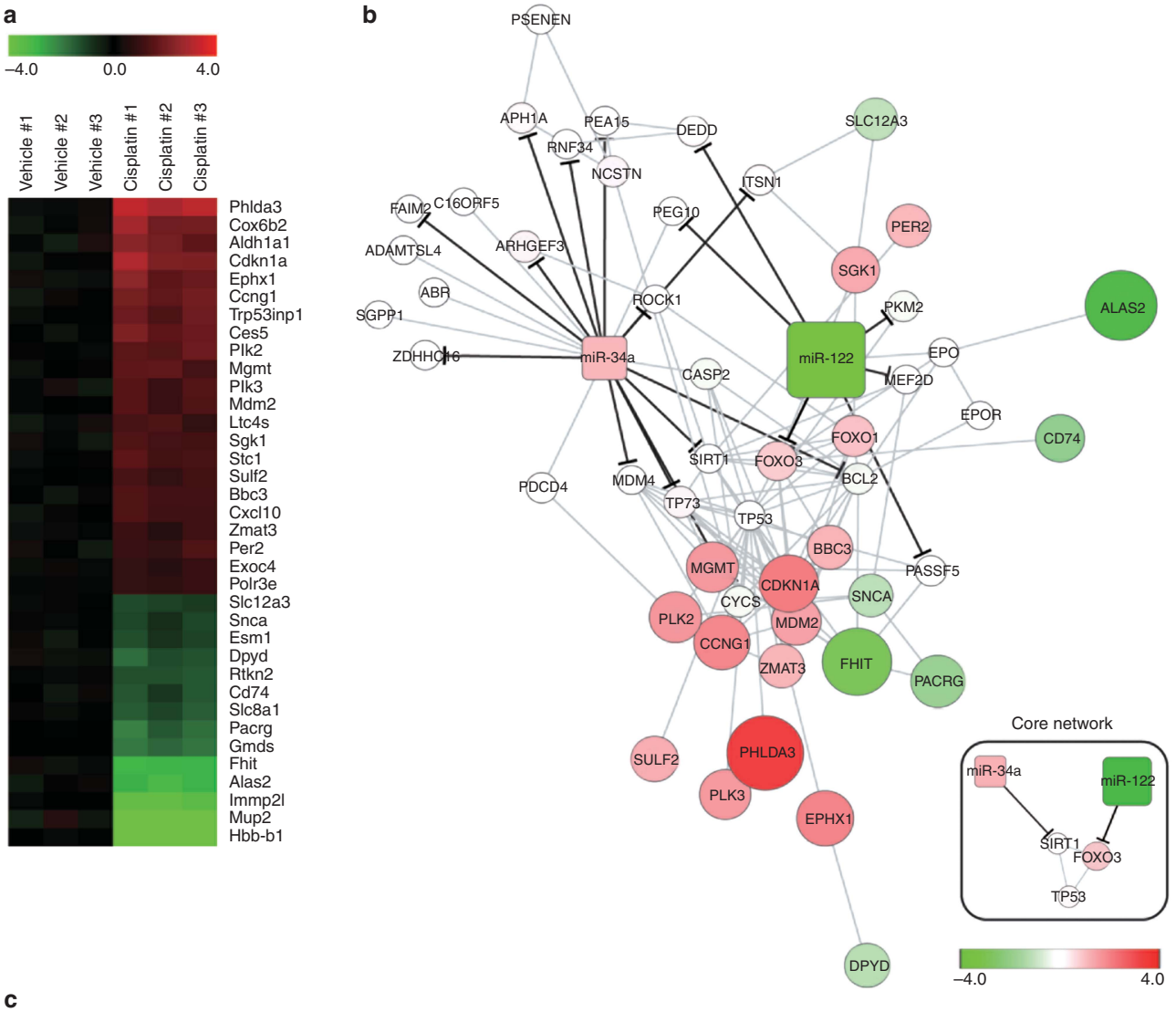

Terms	*P*-value	Z-score
p53 signaling pathway	4.50e–07	4.91
Drug metabolism	8.53e–05	3.76
Cell cycle	0.0022	2.85
Metabolism of xenobiotics by CYP450	0.0024	2.82

Figure 2 | A core microRNA (miRNA)–mRNA network and signaling pathways in acute kidney injury. (**a**) cDNA microarray analyses. Microarrays were performed on RNA samples extracted from the kidney at day 3 after a single administration of vehicle or cisplatin (15 mg/kg) to C57BL/6 mice. Green, downregulation; red, upregulation. (**b**) A network integrating miRNA and transcriptomic data. The size of each node and colors indicate amounts of expression. (**c**) Enriched pathways and Gene Set Enrichment Analysis (GSEA). A functional enrichment analysis was conducted to associate the differentially expressed genes with GO Biological Processes, using the DAVID program. GSEA was performed on the microarray data set obtained from the kidney of mice treated with cisplatin.

along with the outcome of target-prediction program analysis suggested that Foxo3 is likely a key factor governed by the key miRNA regulatory network (Figure 2b). A core network was shown from the integrated network to emphasize molecules interacting with Foxo3 (Figure 2b inset). In addition, the integrative analyses of our database and target prediction pointed out the genes whose expression is necessary for p53-mediated apoptosis (Figure 2b). Consistently, the p53 signaling pathway was most significantly enriched in a functional enrichment analysis (Figure 2c, left). In Gene Set Enrichment Analysis, cisplatin treatment upregulated a subset of genes targeted by p53 ($P = 0.1$; Figure 2c, right).

Foxo3 as a direct target of miR-122

As Foxo3 was an essential target of the identified regulatory network involving miR-122, we next assessed whether miR-122 intervenes with Foxo3 translation. TargetScan program analysis enabled us to find the 3′-UTR of Foxo3 as the target that contains a well-fitted conserved motif matching with the 'seed' sequence of miR-122 (Figure 3a). To assess whether miR-122 inhibits Foxo3, the protein levels were measured in NRK52E cells transfected with either miR-122 mimic or its antisense oligonucleotide (ASO). The miR-122 mimic transfection decreased Foxo3 levels in a dose-dependent manner (Figure 3b, left). miR-122-ASO transfection had the opposite effect (Figure 3b, right). Consistently, the miR-122 mimic prevented luciferase expression from the p-EZX-FOXO3 luciferase construct that comprises the 3′-UTR region of Foxo3 mRNA (Figure 3d). miR-122 mimic transfection had no effect in the assays using a Foxo3 3′UTR-Mut construct that has a mutated binding site. miR-122 mimic or miR-122-ASO transfection slightly, but significantly, changed Foxo3 transcript level (Figure 3e). Our results provide evidence that miR-122 inhibits Foxo3 translation by directly targeting the 3′-UTR of Foxo3 mRNA.

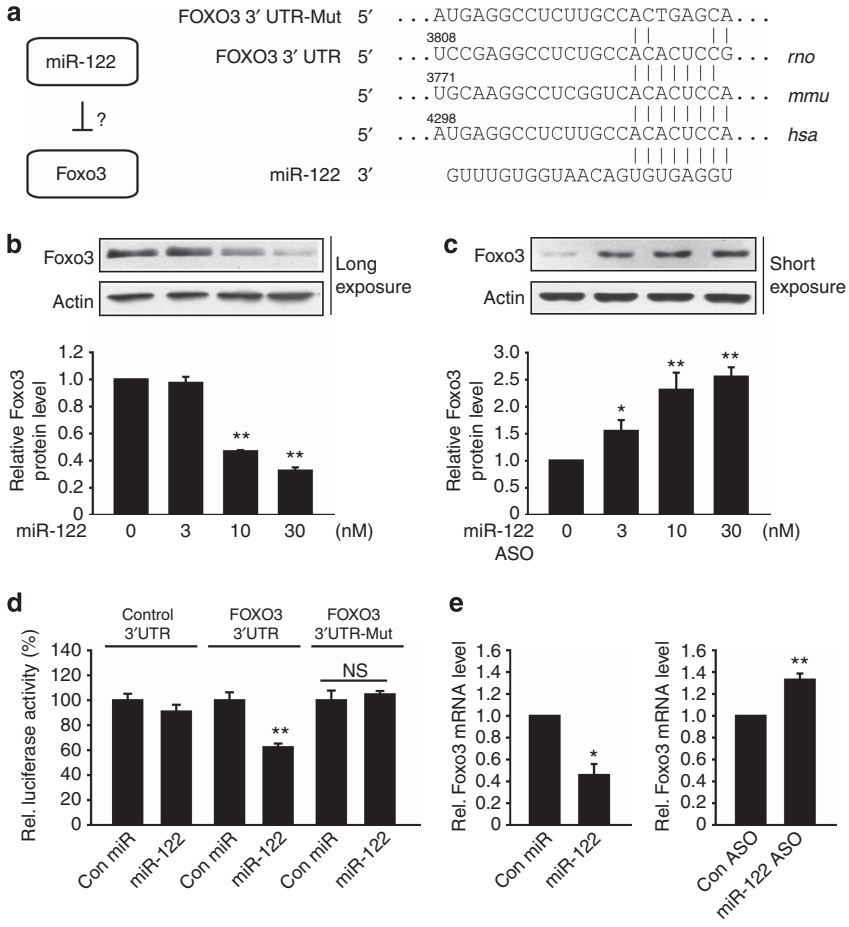

Figure 3 | Direct regulation of Foxo3 by miR-122. (**a**) A sequence of miR-122 and its binding site within the 3′-untranslated region (UTR) of Foxo3. (**b**) Foxo3 repression by miR-122. NRK52E cells were transfected with 3–30 nmol/l miR-122 mimic and were subjected to immunoblotting. (**c**) Foxo3 induction by miR-122-antisense oligonucleotide (ASO). Immunoblotting for Foxo3 was carried out on the lysates of NRK52E cells transfected with 3–30 nmol/l miR-122-ASO. (**d**) Inhibition of Foxo3 3′-UTR reporter activity. Luciferase activity was measured in cells transfected with control miR (con miR) or miR-122 mimic in combination with a reporter comprising a luciferase cDNA fused to the 3′-UTR of control vector (pEZX-Control), Foxo3 (pEZX-FOXO3 3′-UTR), or Foxo3 3′UTR-Mut (pEZX-FOXO3 3′-UTR-Mut). (**e**) The effect of miR-122 modulation on Foxo3 mRNA levels. Quantitative reverse transcription PCR assays were performed to measure Foxo3 mRNA levels in NRK52E cells transfected with miR-122 mimic or ASO. For **b**–**e**, values represent the mean ± s.e.m. (significantly different as compared with control, $^*P < 0.05$, $^{**}P < 0.01$; $N = 3$ separate experiments per group). NS, not significant; Rel., relative.

Foxo3 induction in injured kidney

Although Foxo3 is known as a regulator of apoptosis,[12] the role of Foxo3 in AKI has been scarcely studied. To assess the link between Foxo3 and renal injury, we determined the association of increased levels of Foxo3 with the degree of renal cell death. Kidney function was measured using known blood parameters; blood urea nitrogen and serum creatinine levels were both gradually elevated at day 3 and/or at day 5 after cisplatin treatment (Figure 4a, left). The levels of kidney injury molecule-1 (Kim-1), a well-known biomarker of

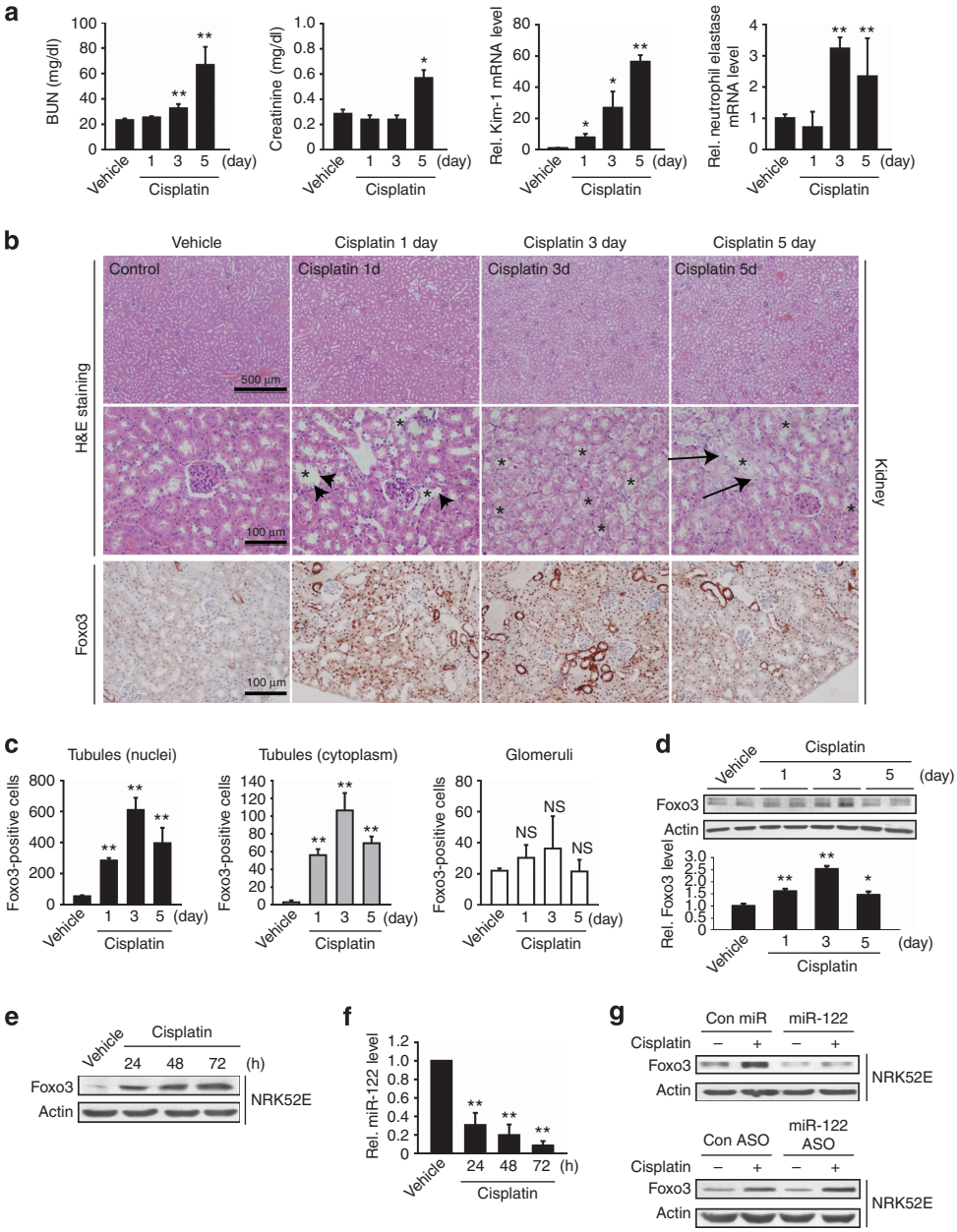

Figure 4 | Foxo3 induction by cisplatin. (**a**) The time-course effect of cisplatin treatment on blood urea nitrogen (BUN), serum creatinine contents, Kim-1 mRNA, and neutrophil elastase mRNA in the kidney. (**b**) Hematoxylin and eosin (H&E) staining and immunohistochemical analysis for Foxo3. Asterisks indicated desquamation of the tubular epithelium. Arrowheads indicate flattened tubular epithelium, whereas arrows indicate nuclear swelling and vacuolization of the tubular epithelium in necrotizing tubular epithelia. Bar = 500 μm in the upper column and 100 μm in the middle and lower columns. (**c**) Quantification of Foxo3-positive cells in tubules (nuclear and cytoplasmic) or glomeruli. (**d**) The effect of cisplatin treatment on Foxo3. Foxo3 levels in the kidney were measured by immunoblotting at the indicated times after an intraperitoneal injection of cisplatin in C57BL/6 mice. For **a**, **c** and **d**, values represent the mean ± s.e.m. (significantly different as compared with vehicle-treated control (Con), $^{*}P<0.05$, $^{**}P<0.01$; $N=4$ per group). (**e**) The effect of cisplatin on Foxo3 in NRK52E cells. Immunoblotting was performed on the lysates of NRK52E cells treated with 30 μmol/l cisplatin for the indicated times. (**f**) Decrease in miR-122 in NRK52E cells treated with cisplatin. Data represent the mean ± s.e.m. of three replicates (treatment mean significantly different from the mean of vehicle-treated Con, $^{**}P<0.01$). (**g**) The effect of miR-122 modulation on Foxo3. NRK52E cells were transfected with 10 nmol/l miR-122 mimic or antisense oligonucleotide (ASO), followed by treatment with 30 μmol/l cisplatin for 48 h. NS, not significant; Rel. relative.

AKI,[13] were also increased, which matched the progressive renal damage elicited by cisplatin (Figure 4a, middle). Cisplatin treatment promoted infiltration of inflammatory cells (neutrophil and macrophage) in the kidney, as indicated by increases of neutrophil elastase and F4/80, respectively (Figure 4a, right; and Supplementary Figure S1A online). Consistently, tumor necrosis factor-α and intercellular adhesion molecule mRNA levels were increased (Supplementary Figure S1B and C online). Levels of CD3ε and CD19 (indicators of T cell and B cell) were marginally changed (Supplementary Figure S1A online).

Histopathological and immunohistochemical assays supported the concept that increased levels of Foxo3 contributed to tubular cell injury (Figure 4b). Quantification of immunohistochemical data confirmed Foxo3 increase in both nuclei and cytoplasm (Figure 4c). Foxo3 levels were elevated at day 1 or day 3 after cisplatin treatment, and slightly returned to control levels at day 5 (Figure 4d). In addition, cisplatin treatment decreased NRK52E cell viability (data not shown), which was accompanied not only by Foxo3 induction but also by decrease in miR-122 (Figure 4e and f). To link between miR-122 repression and Foxo3 induction in the tubular cell injury, the effect of miR-122 mimic or ASO transfection on Foxo3 expression was examined in NRK52E cells treated with cisplatin. miR-122 mimic transfection abrogated the ability of cisplatin to induce Foxo3, whereas that with miR-122-ASO fortified it (Figure 4g). These data indicate that Foxo3 induced by decrease in miR-122 may contribute to cisplatin-induced kidney toxicity.

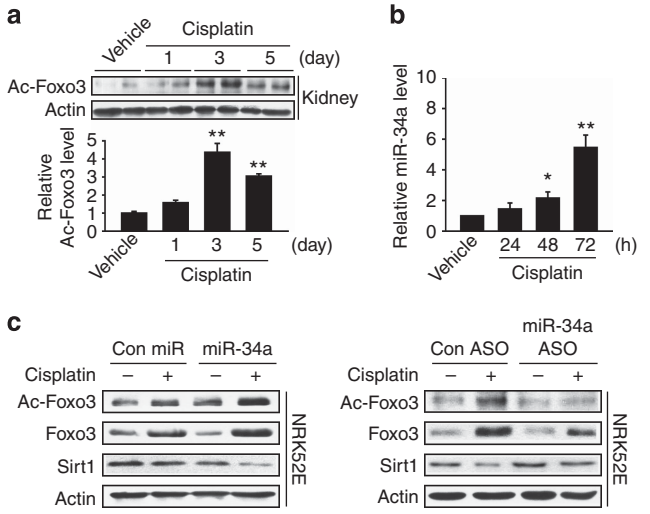

Figure 5 | Role of miR-34a in the acetylation of Foxo3 by cisplatin. (**a**) Acetylated Foxo3 levels in the kidney. Immunoblotting for acetyl-lysine was performed on Foxo3 immunoprecipitates prepared at the indicated times. Values represent the mean ± s.e.m. (significantly different as compared with vehicle-treated control (Con), $^{**}P<0.01$; $N=4$ per group). (**b**) Induction of miR-34a by cisplatin in NRK52E cells. Data represent the mean ± s.e.m. of three replicates (treatment mean significantly different from the mean of vehicle-treated Con, $^{*}P<0.05$, $^{**}P<0.01$). (**c**) The effect of miR-34a modulations on Foxo3. The cells were similarly treated as described in Figure 4g.

Foxo3 activation by miR-34a

On the basis of the established network, we next assessed the effect of miR-34a on the expression of key molecule(s) interacting with Foxo3. As miR-34a inhibits the expression of Sirt1 responsible for deacetylation of Foxo3,[12,14] we monitored acetyl modification of Foxo3 in response to cisplatin treatment. Acetylated Foxo3 levels were increased by cisplatin in parallel with progressive renal damage (Figure 5a). A time-dependent increase in miR-34a level by cisplatin was also verified in NRK52E cells (Figure 5b). As expected, cisplatin treatment increased the levels of acetylated and total forms of Foxo3 (Figure 5c, left). miR-34a mimic transfection in combination with cisplatin treatment further enhanced the acetylated or total form of Foxo3 levels. miR-34a-ASO transfection resulted in the opposite effect (Figure 5c, right). These results showed that miR-34a upregulated by cisplatin may contribute to the activation of Foxo3 presumably via Sirt1 repression.

Foxo3 as a bridge molecule to activate the p53 signaling pathway

Foxo3 has been shown to directly bind p53 and activate p53-dependent apoptosis.[15,16] Having identified Foxo3 as a bridge protein between dysregulated miRNAs and p53 signaling pathway in tubular cell injury, we confirmed the functional role of Foxo3 induced by cisplatin in the activation of p53. Treatment of NRK52E cells with cisplatin facilitated the association of Foxo3 and p53 as a function of time, being in parallel with the accumulation of p53 and Bax (Figure 6a). Abrogation of the basal and cisplatin-inducible expression of p53 by the knockdown of Foxo3 verified the key role of Foxo3 in maintaining upregulated levels of p53 (Figure 6b). Consistently, miR-122 mimic transfection diminished p53 and Bax levels in NRK52E cells treated with cisplatin, whereas that with miR-122-ASO exerted the opposite effect (Figure 6c). In addition, miR-34a mimic transfection promoted both the basal and the inducible expression of p53 and Bax (Figure 6d). miR-34a-ASO transfection antagonized the ability of cisplatin to increase p53 and Bax levels. All of these results strongly support the conclusion that the increased expression and activation of Foxo3 elicited by toxicant-induced miRNA dysregulation has a role in triggering the p53 signaling pathway.

Phlda3 as an effector molecule activated by p53 in AKI

As a continuing effort to find the molecule responsible for tubular cell death downstream from p53, we sought to examine the levels of downstream effector molecules in the core network (Figure 7a). In quantitative reverse transcription-PCR assays, cisplatin treatment substantially upregulated the expression of Phlda3 mRNA and other p53 target transcripts (Figure 7b). Of them, Phlda3 showed the highest mRNA fold change and the lowest *P*-value in the kidney

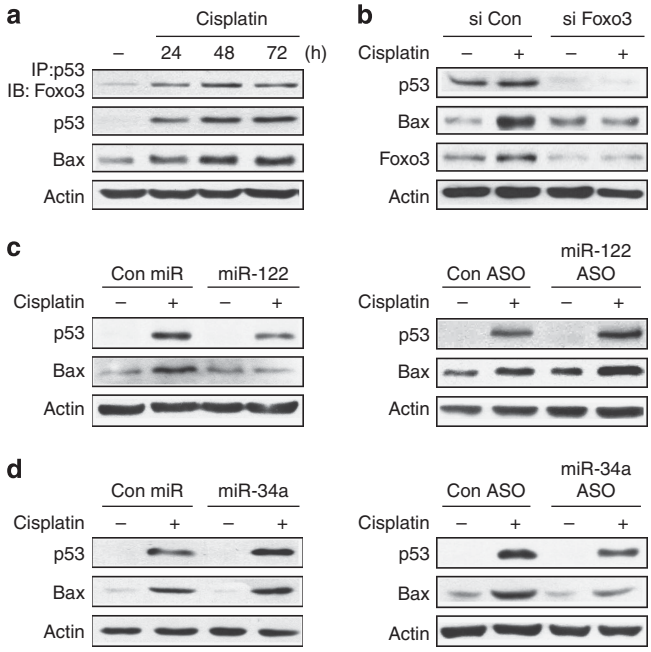

Figure 6 | The effects of miR-122 or -34a modulations on Foxo3 and p53 activation by cisplatin. (**a**) Binding of Foxo3 and p53 for activation. Immunoblotting (IB) for Foxo3 was performed on p53 immunoprecipitates (IPs) from NRK52E cells treated with 30 μmol/l cisplatin for the indicated times. (**b**) Inhibition of p53 by small interfering RNA (siRNA) knockdown of Foxo3. NRK52E cells were transfected with a siRNA directed against Foxo3 followed by treatment with 30 μmol/l cisplatin for 48 h. (**c**) The effect of miR-122 mimic or antisense oligonucleotide (ASO) on p53. (**d**) The effect of miR-34a mimic or ASO on p53.

injured by cisplatin. As the structure of Phlda3 is similar to the PH-domain,[17] Phlda3 may interfere with binding of activating Akt to the plasma membrane.[18,19] In a time-course study, p53 or Phlda3 levels in the kidney were also elevated by cisplatin treatment, which caused gradual decreases in p-Akt levels (Figure 7c). To associate Phlda3 and tubular injury by cisplatin, we measured Phlda3- and terminal deoxynucleotidyl transferase dUTP nick end labeling (TUNEL)-positive cell numbers using serial kidney sections. Cisplatin treatment markedly increased TUNEL-positive cell numbers (Figure 7d). In the samples, TUNEL-positive cells were detected to a greater extent in Phlda3-positive cells than in Phlda3-negative ones, supporting the notion that Phlda3 induced by cisplatin may contribute to tubular cell death.

In a NRK52E cell model, cisplatin treatment increased the expression of Phlda3, which matched decreases in p-Akt at 48 and 72 h after an adaptive increase at 24 h (Figure 7e). In the cells treated with cisplatin (48 h), the ability of Phlda3 to antagonize Akt phosphorylation was verified by the increase in p-Akt level after knockdown of Phlda3 (Figure 7f). As expected, miR-122 transfection resulted in the opposite effect (Figure 7g). Our results demonstrate that Phlda3 substantially induced by cisplatin downstream from p53 may facilitate tubular cell death by diminishing Akt activity.

Changes in cell viability by modulations of the targets identified

Finally, we monitored whether modulations of miR-122 and/or -34a levels affect the degree of cisplatin-induced cell death *in vitro*. miR-122-ASO transfection further decreased the viability of NRK52E cells as compared with cisplatin treatment alone, whereas that with miR-122 mimic increased it (Figure 8a). When the cells were transfected with either miR-34a mimic or miR-34a-ASO, cell viability was significantly changed (Figure 8b). Combined treatment with miR-122-ASO and miR-34a mimic further decreased the viability of cells in response to cisplatin (Figure 8c). Also, silencing of Foxo3 completely prevented cisplatin-induced cytotoxicity, whereas that of Phlda3 partially did so (Figure 8d and e). In the rescue assay, the protective effect of miR-122 against cisplatin was diminished by transfection with a Foxo3 construct lacking the 3′UTR (Figure 8f). These results support the conclusion that Foxo3 induced and activated by miR-122 and -34a dysregulation contributes to acute tubular injury by fortifying the p53 signaling pathway (Figure 8g).

DISCUSSION

Many '-omics' studies have been conducted to elucidate the molecular pathology. Nonetheless, the underlying basis and the cascade pathway leading to renal injury are only partially known from the databases. Moreover, miRNA expression profiles accounting for AKI had not been identified. Our miRNA microarray data shown in the present study demonstrate for the first time that miR-122 levels were most markedly decreased in the kidney injured by cisplatin treatment throughout the time points examined (1–5 days). Our finding also showed a distinct increase in the level of miR-34a, raising the hypothesis that AKI induced by toxicant might be controlled by miR-122 and -34a dysregulation.

An important finding of the present study is the discovery of a core miRNA–mRNA network that associates Foxo3 with the process of toxicant-induced injury. Our integrated approach may serve as a major step forward as compared with the commonly used transcriptome-based approach because the identified miRNA and mRNA network was of value in defining Foxo3 as the key molecule that is posttranscriptionally and posttranslationally activated and triggers the pathway leading to AKI. In association with the discovery of Foxo3 as a bridge molecule, the present work enabled us to extract the enriched pathways associated with kidney injury, which included the p53 signaling pathway, cell cycle, and CYP450 metabolism of xenobiotics. Because cisplatin has an effect on cell-cycle progression for cancer therapy, the expression of cell-cycle–associated genes was significantly changed. CYP450 and metabolism pathways were also affected probably because cisplatin is metabolized in the liver and kidney.

In the present study, we revealed the new function of miR-122 as a direct suppressor of Foxo3 mRNA translation, as shown by its ability to inhibit Foxo3 expression and decrease Foxo3 3′-UTR reporter activity. The role of miR-122 in

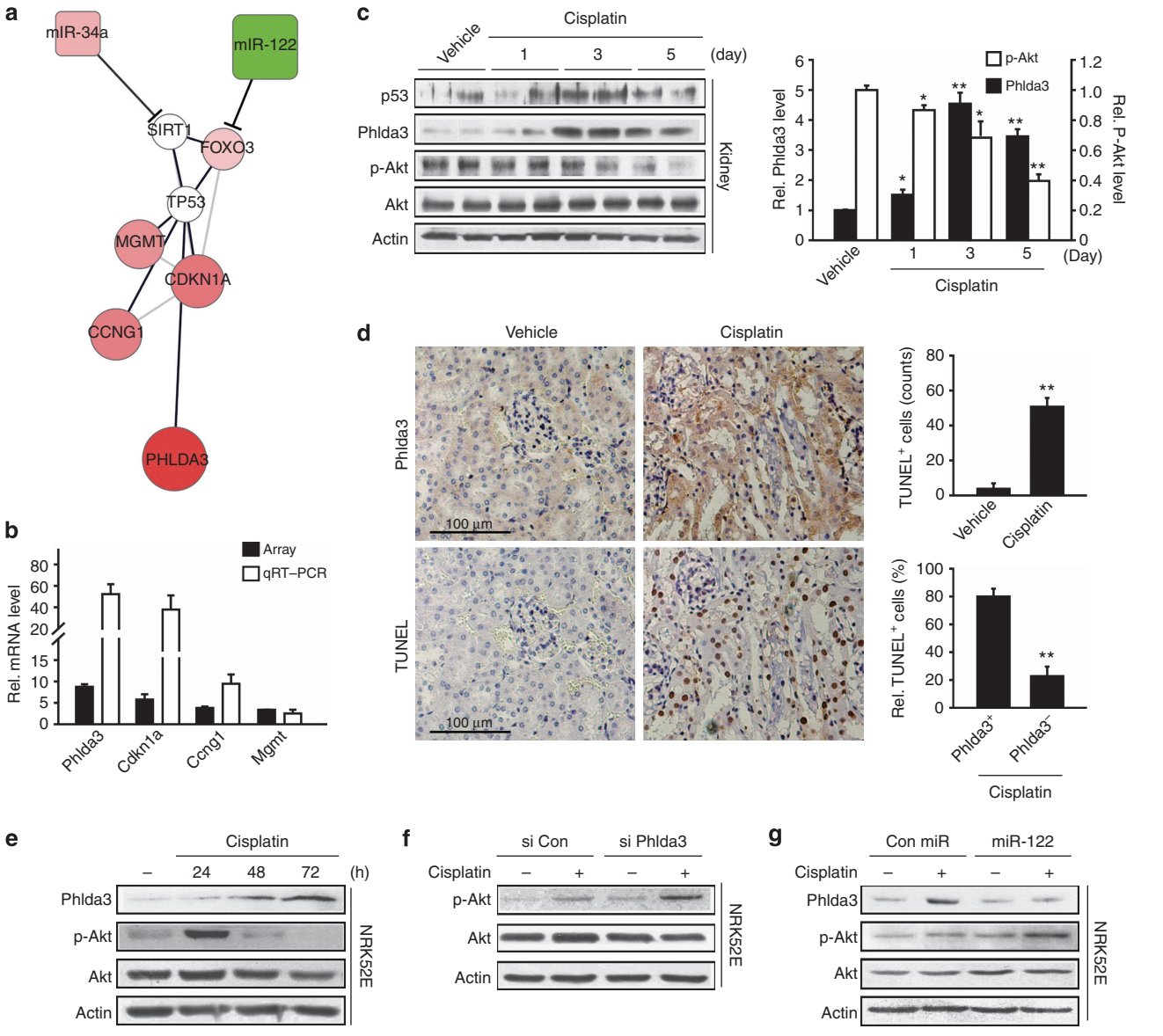

Figure 7 | A core integrative network and interacting molecules. (**a**) A core network of microRNA (miRNA) and mRNA leading to the induction of Phlda3. (**b**) Upregulation of p53 target genes in the kidney of mice treated with cisplatin as described in Figure 1a. (**c**) Immunoblotting for p53, Phlda3, and p-Akt in the kidney homogenates. Data represent the mean ± s.e.m. (treatment mean significantly different from the mean of vehicle-treated control, $^{*}P<0.05$, $^{**}P<0.01$; $N=4$ per group). (**d**) Immunohistochemical analysis for Phlda3 and terminal deoxynucleotidyl transferase dUTP nick end labeling (TUNEL) staining in the kidney of mice treated with cisplatin as described in Figure 1a. (**e**) Immunoblotting for Phlda3 and p-Akt in NRK52E cells treated with cisplatin (30 μmol/l). (**f**) The effect of Phlda3 knockdown on p-Akt. NRK52E cells were transfected with small interfering (si) RNA directed against Phlda3, followed by treatment with 30 μmol/l cisplatin for 48 h. (**g**) The effect of miR-122 mimic treatment on Phlda3 and p-Akt. Con, control; qRT-PCR, quantitative reverse transcription-PCR; Rel., relative.

regulating Foxo3 was fortified by the result obtained using miR-122-ASO. Our findings represent the first evidence that decrease in miR-122 causes the induction of Foxo3 during AKI. The causal effect of Foxo3 on tubular cell death was strengthened by the finding that cisplatin treatment increased Foxo3 in a cell model, which was reversed by the miR-122 mimic and enhanced by miR-122-ASO. Consistently, our results confirmed an increase in Foxo3 levels *in vivo*: Foxo3 induction was also detectible in the immunohistochemical analysis, implying that Foxo3 may serve as a marker of tubular cell injury. Increase in Foxo3 was observed in tubules, but not in glomeruli (Figure 4c), although injuries were found in both (Supplementary Figure S2 online), suggesting the notion that Foxo3 controlled by the proposed integrative network is induced in a cell-type–specific manner.

It has been extensively studied that miR-122 is highly abundant in the liver and is implicated in liver diseases.[20,21] Nevertheless, the functional role of miR-122 in kidney disease

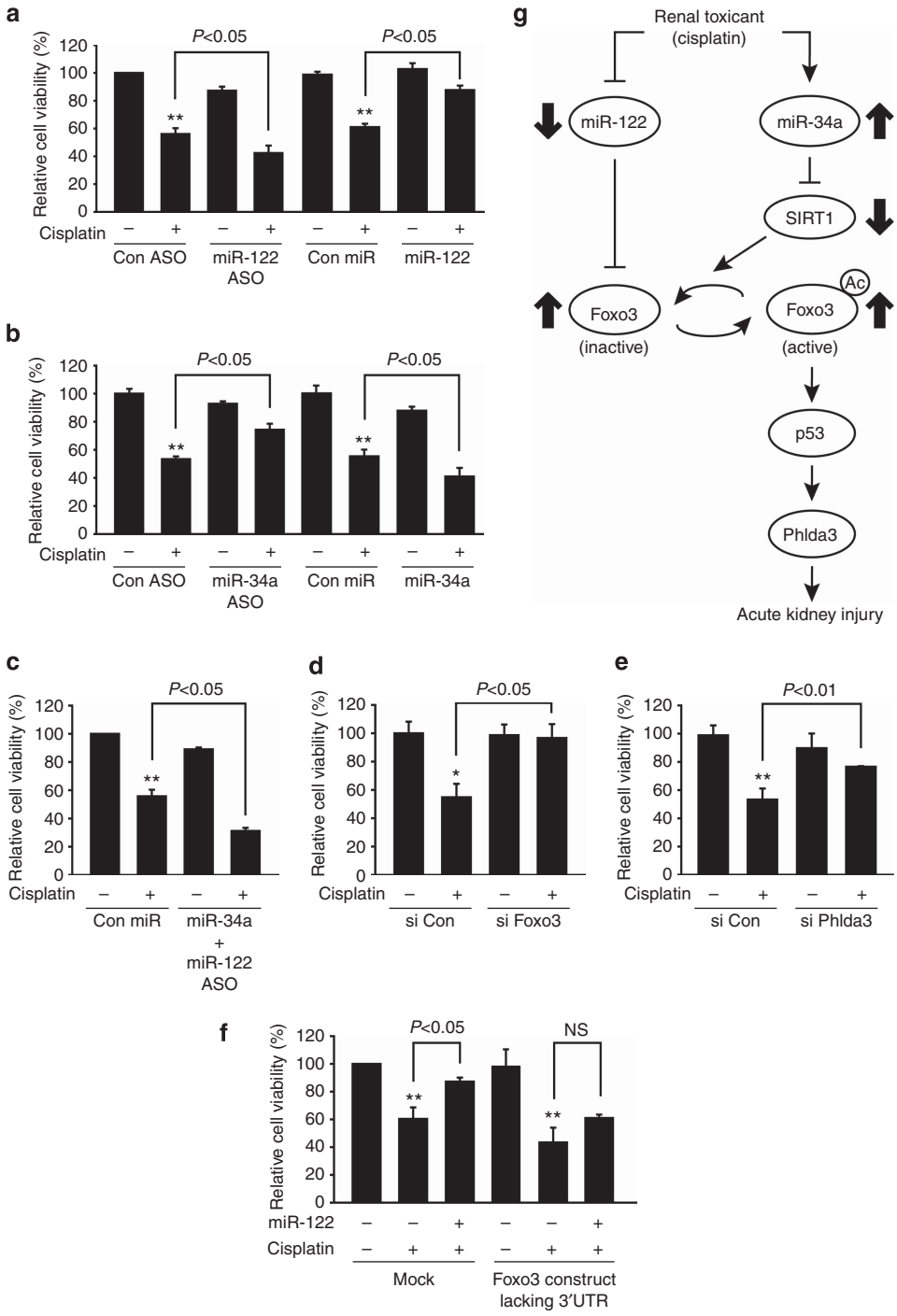

Figure 8 | Cell viability after modulations of miR-122 and -34a, or Foxo3 and Phlda3. (**a**) The effect of miR-122 on cisplatin-induced cell death. NRK52E cells were transfected with miR-122 mimic or antisense oligonucleotide (ASO), followed by treatment with 30 μmol/l cisplatin for 48 h. (**b**) The effect of miR-34a on cisplatin-induced cell death. (**c**) The effect of combined treatment with miR-122-ASO and miR-34a mimic. (**d**) Decrease in cisplatin-induced cell death by Foxo3 knockdown. NRK52E cells were transfected with a small interfering RNA directed against Foxo3, followed by treatment with 30 μmol/l cisplatin for 72 h. (**e**) Improvement in cell survival by Phlda3 knockdown. (**f**) The effect of transfection with a Foxo3 construct lacking the 3′-untranslated region (UTR) on the cytoprotective effect of miR-122. (**g**) A proposed pathway by which nephrotoxicant elicits AKI. For **a**–**f**, data represent the mean ± s.e.m. of four replicates (treatment mean significantly different from that of vehicle-treated control (Con), $^{*}P<0.05$, $^{**}P<0.01$).

has been scarcely explored. In recent studies, miR-122 has been shown to be upregulated in renal cancer,[22,23] which may account for the progression of RCC growth and proliferation. Despite the effect of increased levels of miR-122 on renal cancer biology, the role of miR-122 in the physiology of normal kidney cells was unknown. Another important

finding of the present study is that decrease in miR-122 contributed to tubular cell injury on cisplatin treatment. As the basal miR-122 levels might be greater in tubules than in glomeruli ($P<0.1$; Supplementary Figure S3 online), miR-122 dysregulation may be more predominant in tubules. Overall, miR-122 may function as a mediator that controls tubular cell viability despite its lesser basal expression in the kidney than in the liver, suggestive of its potential as a therapeutic means to prevent and/or treat toxic nephropathy.

In several toxic challenges, miR-34a has been shown to be induced.[24,25] In addition, miR-34a is a target gene of p53 activation during DNA damage, implying that increase in miR-34a may reflect the ensuing apoptosis.[25] miR-34a represses Sirt1, a deacetylase that activates Foxo3.[12,26,27] In our findings, miR-34a was also distinctly elevated in the kidney after cisplatin treatment. As increase in miR-34a activates Foxo3 by suppressing Sirt1, it is highly likely that posttranslational modification of Foxo3 due to an increase in miR-34a favors a shift in tubular cell viability toward cell-cycle arrest or apoptosis.

An active form of Foxo3 induces p53-dependent apoptosis by cytoplasmic accumulation and stabilization of p53.[28] Two regions within Foxo3 (FH and CR3 domains) interact with the DNA-binding domain of p53.[29] It is well recognized that p53 becomes activated in response to a myriad of stress.[30] In kidney tubules, the accumulation of p53 leads to cell-cycle arrest and apoptosis.[31,32] In our results, Foxo3 induced by cisplatin promoted its interaction with p53, enhancing p53 stability. Consistently, Foxo3 induction by cisplatin precedes p53 stabilization and activation. Our data showing Foxo3–p53 binding or p53 accumulation as a consequence of miR-122 and -34a dysregulation strengthens the regulatory function of the identified miRNA–mRNA core network in the process of AKI.

Drug-induced acute renal failure is encountered in a growing number of patients because of a more aggressive diagnostic or therapeutic approach in an aging and multi-medicated patient population that is increasingly vulnerable.[33,34] Although chemical-induced AKI is encountered in many people because of medications or exposure to environmental toxicants,[3] limited information had been available on the mechanism of toxic nephropathy and the responsible molecules.[35] In the present study, the results of the cDNA microarray and the enriched pathways obtained from the microarray data included not only the activation of p53 but also the large induction of Phlda3, enabling us to find Phlda3 as one of the effector molecules causing tubular cell death. This contention was further supported by the observation that Phlda3 contributes to tubular cell death in cell-based assays, as also strengthened by the *in vivo* results of immunohistochemical analysis and TUNEL staining.

In an effort to generalize the pathological relevance of the proposed network in renal injury, we additionally employed other toxicants and monitored miRNAs and target gene expression levels. Treatment with either doxorubicin or gentamicin dysregulated miR-122 and -34a in the kidney of mice as did cisplatin treatment, which matched not only with the severities of renal injury but also with the increases in Foxo3 and p53 (Supplementary Figure S4A–C online). Our data strengthen the contention that renal toxicants induce tubular injuries probably through the pathways of the integrative miRNA–mRNA network.

Collectively, the results shown here demonstrate that dysregulation of miR-122 and -34a has a critical role in acute renal tubular injury caused by toxicants, identifying Foxo3 as a key molecule bridging to augment the p53 signaling pathway. This idea was fortified by the abilities of exogenous miR-122 and -34a mimics or inhibitors to alter p53 and Bax levels in cell-based assays. Moreover, our findings strongly support the conclusion that dysregulation of miR-122 and -34a leads to Phlda3-mediated tubular injury, implying that modulations of the identified miRNAs, bridging molecules, and/or effector molecules could be the mechanism with which to prevent or treat AKI elicited by nephrotoxicants.

MATERIALS AND METHODS

Additional details regarding the materials and methods are provided in Supplementary Information online.

Animal treatment

Animal experiments were conducted under the guidelines and ethical approvals of the Institutional Animal Use and Care Committee at Seoul National University. Male C57BL/6 mice (9 weeks old) were purchased from Samtako Company (Osan, Korea) and housed under filtered, pathogen-free air, with food and water available *ad libitum*. After the mice were injected with a single dose of cisplatin (15 mg/kg, i.p.), doxorubicin (20 mg/kg, i.p.), and gentamicin (250 mg/kg, i.p.), the cortices of kidney tissues were taken for biochemical assays.

miRNA and cDNA microarray analyses

The mirVana miRNA isolation kit (Ambion, Austin, TX) was used for total RNA isolation according to the manufacturer's protocol. miRNA microarray analysis was performed using the Agilent mouse miRNA microarray (Agilent, Santa Clara, CA), which was based on Sanger miRbase release 15.0 (http://www.mirbase.org).

For cDNA microarray analyses, the integrity of total RNA extracted from mouse kidney was assessed using Bioanalyzer 2100 (Agilent). The RNA integrity number was 10 for all samples. A measure of 500 ng of high-quality total RNA was amplified with a TotalPrep amplification kit (Ambion), and 750 ng of amplified cRNA was hybridized to the Illumina MouseWG-6 expression beadchip (Illumina, San Diego, CA) for 16 h. The hybridized array was scanned with a BeadArray Reader (Illumina). The probe intensities were normalized at log2 scale using quantile normalization in beadarray 1.6 (http://www.bioconductor.org), an R/Bioconductor package. The microarray data were deposited in the GEO database before submission (accession number: GSE35257).

Real-time PCR assays

Total RNA for quantitative reverse transcription-PCR was extracted using Tri-Reagent (Molecular Research Center, Cincinnati, OH). Quantitative reverse transcription-PCR was carried out according to the manufacturer's instructions using a Light CyclerDNA master SYBR green-I kit (Light-Cycler 2.0, Roche, Mannheim, Germany) as

described previously.[36] The details and primer information are in Supplementary Information online.

Bioinformatic analyses

Differentially expressed genes by cisplatin treatment were statistically selected as the genes with *t*-test *P*-values less than 0.01 with a fold change >2. Statistically enriched signaling pathways of clustered differentially expressed genes were ranked and categorized according to the Kyoto Encyclopedia of Genes and Genomes pathway using DAVID software.[37] Targetscan 6.2 database (http://www.targetscan.org) was used to predict mRNAs possibly regulated by the differentially expressed miRNAs. Gene interaction network between the clustered differentially expressed genes was achieved by STRING 9.0 (http://string-db.org) and visualized by Cytoscape software.[38,39]

DISCLOSURE

All the authors declared no competing interests.

ACKNOWLEDGMENTS

This work was financially supported by the Korea Ministry of Food and Drug Safety in 2010–2012 (10182KFDA992).

SUPPLEMENTARY MATERIAL

Figure S1. The effects of cisplatin treatment on kidney inflammation.
Figure S2. TUNEL staining in tubules and glomeruli.
Figure S3. qRT-PCR assays for miR-122 and -34a in tubules and glomeruli.
Figure S4. The effects of other nephrotoxicants on miR-122, miR-34a, Foxo3, and p53 levels.
Table S1. The candidate target genes of miR-122 that are associated with apoptosis regulation.
Table S2. The candidate target genes of miR-34a that are associated with apoptosis regulation.
Supplementary material is linked to the online version of the paper at http://www.nature.com/ki

REFERENCES

1. Himmelfarb J, Ikizler TA. Acute kidney injury: changing lexicography, definitions, and epidemiology. *Kidney Int* 2007; **71**: 971–976.
2. Uchino S, Kellum JA, Bellomo R *et al.* Acute renal failure in critically ill patients: a multinational, multicenter study. *JAMA* 2005; **294**: 813–818.
3. Vilay AM, Wong CS, Schrader RM *et al.* Indicators for serious kidney complications associated with toxic exposures: an analysis of the National Poison Data System. *Clin Toxicol (Phila)* 2013; **51**: 96–105.
4. Bagga S, Bracht J, Hunter S *et al.* Regulation by let-7 and lin-4 miRNAs results in target mRNA degradation. *Cell* 2005; **122**: 553–563.
5. Ho J, Kreidberg JA. The long and short of microRNAs in the kidney. *J Am Soc Nephrol* 2012; **23**: 400–404.
6. Chandrasekaran K, Karolina DS, Sepramaniam S *et al.* Role of microRNAs inkidney homeostasis and disease. *Kidney Int* 2012; **81**: 617–627.
7. Pandey P, Brors B, Srivastava PK *et al.* Microarray-based approach identifies microRNAs and their target functional patterns in polycystic kidney disease. *BMC Genomics* 2008; **9**: 624.
8. Krupa A, Jenkins R, Luo DD *et al.* Loss of MicroRNA-192 promotes fibrogenesis in diabetic nephropathy. *J Am Soc Nephrol* 2010; **21**: 438–447.
9. Kato M, Arce L, Wang M *et al.* A microRNA circuit mediates transforming growth factor-beta1 autoregulation in renal glomerular mesangial cells. *Kidney Int* 2011; **80**: 358–368.
10. Laloo B, Simon D, Veillat V *et al.* Analysis of post-transcriptional regulations by a functional, integrated, and quantitative method. *Mol Cell Proteomics* 2009; **8**: 1777–1788.
11. Pabla N, Dong Z. Cisplatin nephrotoxicity: mechanisms and renoprotective strategies. *Kidney Int* 2008; **73**: 994–1007.
12. Giannakou ME, Partridge L. The interaction between FOXO and SIRT1: tipping the balance towards survival. *Trends Cell Biol* 2004; **14**: 408–412.
13. Vaidya VS, Ferguson MA, Bonventre JV. Biomarkers of acute kidney injury. *Annu Rev Pharmacol Toxicol* 2008; **48**: 463–493.
14. Yamakuchi M, Ferlito M, Lowenstein CJ. miR-34a repression of SIRT1 regulates apoptosis. *Proc Natl Acad Sci USA* 2008; **105**: 13421–13426.
15. Chung YM, Park SH, Tsai WB *et al.* FOXO3 signalling links ATM to the p53 apoptotic pathway following DNA damage. *Nat Commun* 2012; **3**: 1000.
16. You H, Mak TW. Crosstalk between p53 and FOXO transcription factors. *Cell Cycle* 2005; **4**: 37–38.
17. Saxena A, Morozov P, Frank D *et al.* Phosphoinositide binding by the pleckstrin homology domains of Ipl and Tih1. *J Biol Chem* 2002; **277**: 49935–49944.
18. Datta K, Franke TF, Chan TO *et al.* AH/PH domain-mediated interaction between Akt molecules and its potential role in Akt regulation. *Mol Cell Biol* 1995; **15**: 2304–2310.
19. Kawase T, Ohki R, Shibata T *et al.* PH domain-only protein PHLDA3 is a p53-regulated repressor of Akt. *Cell* 2009; **136**: 535–550.
20. Lagos-Quintana M, Rauhut R, Yalcin A *et al.* Identification of tissue-specific microRNAs from mouse. *Curr Biol* 2002; **12**: 735–739.
21. Girard M, Jacquemin E, Munnich A *et al.* miR-122, a paradigm for the role of microRNAs in the liver. *J Hepatol* 2008; **48**: 648–656.
22. Zhou L, Chen J, Li Z *et al.* Integrated profiling of microRNAs and mRNAs: microRNAs located on Xq27.3 associate with clear cell renal cell carcinoma. *PLoS One* 2010; **5**: e15224.
23. Osanto S, Qin Y, Buermans HP *et al.* Genome-wide microRNA expression analysis of clear cell renal cell carcinoma by next generation deep sequencing. *PLoS One* 2012; **7**: e38298.
24. Ghawanmeh T, Thunberg U, Castro J *et al.* miR-34a expression, cell cycle arrest and cell death of malignant mesothelioma cells upon treatment with radiation, docetaxel or combination treatment. *Oncology* 2011; **81**: 330–335.
25. Chang TC, Wentzel EA, Kent OA *et al.* Transactivation of miR-34a by p53 broadly influences gene expression and promotes apoptosis. *Mol Cell* 2007; **26**: 745–752.
26. Brunet A, Sweeney LB, Sturgill JF *et al.* Stress-dependent regulation of FOXO transcription factors by the SIRT1 deacetylase. *Science* 2004; **303**: 2011–2015.
27. Motta MC, Divecha N, Lemieux M *et al.* Mammalian SIRT1 represses forkhead transcription factors. *Cell* 2004; **116**: 551–563.
28. You H, Yamamoto K, Mak TW. Regulation of transactivation-independent proapoptotic activity of p53 by FOXO3a. *Proc Natl Acad Sci USA* 2006; **103**: 9051–9056.
29. Wang F, Marshall CB, Yamamoto K *et al.* Biochemical and structural characterization of an intramolecular interaction in FOXO3a and its binding with p53. *J Mol Biol* 2008; **384**: 590–603.
30. Boulon S, Westman BJ, Hutten S *et al.* The nucleolus under stress. *Mol Cell* 2010; **40**: 216–227.
31. Dagher PC. Apoptosis in ischemic renal injury: roles of GTP depletion and p53. *Kidney Int* 2004; **66**: 506–509.
32. Molitoris BA, Dagher PC, Sandoval RM *et al.* siRNA targeted to p53 attenuates ischemic and cisplatin-induced acute kidney injury. *J Am Soc Nephrol* 2009; **20**: 1754–1764.
33. Chronopoulos A, Cruz DN, Ronco C. Hospital-acquired acute kidney injury in the elderly. *Nat Rev Nephrol* 2010; **6**: 141–149.
34. Evenepoel P. Toxic nephropathy due to drugs and poisons. In: Jörres A, Ronco C, Kellum JA (eds). *Management of Acute Kidney Problems*. Springer Publications: New York, 2010, pp 317–328.
35. Faubel S, Chawla LS, Chertow GM *et al.* Ongoing clinical trials in AKI. *ClinJ Am Soc Nephrol* 2012; **7**: 861–873.
36. Lee CG, Kim YW, Kim EH *et al.* Farnesoid X receptor protects hepatocytes from injury by repressing miR-199a-3p, which increases levels of LKB1. *Gastroenterology* 2012; **142**: 1206–1217.
37. Huang da W, Sherman BT, Lempicki RA. Systematic and integrative analysis of large gene lists using DAVID bioinformatics resources. *Nat Protoc* 2009; **4**: 44–57.
38. Szklarczyk D, Franceschini A, Kuhn M *et al.* The STRING database in 2011: functional interaction networks of proteins, globally integrated and scored. *Nucleic Acids Res* 2011; **39**: D561–D568.
39. Smoot ME, Ono K, Ruscheinski J *et al.* Cytoscape 2.8: new features for data integration and network visualization. *Bioinformatics* 2011; **27**: 431–432.